Supporting Information

Nickel foam deposited with borophene sheets used as a self-supporting binder-free anode of lithium-ion batteries

Ting Bi,[a] Junzhe Zhang,[a] Mei Wang,[a] Liyong Wang,[a] Jingpeng Chen,[b] Shengliang Hu,[a] Chenmeng Chen,[b] and Huiqi Wang*[a]

[a] *School of Energy and Power Engineering & School of Materials Science and Engineering, North University of China, Taiyuan 030051, P. R. China*

E-mail: hqiwang@nuc.edu.cn

[b] *CAS Key Laboratory of Carbon Materials, Institute of Coal Chemistry, Chinese Academy of Sciences, Taiyuan 030001, P. R. China*

Optimization of preparation process. The preparation of boron source and ultrasonic cleaning of nickel foam were the same as above. The reaction of high temperature annealing of nickel foam and deposition of borophene was carried out in one procedure. The experimental parameters such as temperature value, heating rate and holding time in the two temperature zones were shown in Figure S1. The T_1 temperature zone was also heated to 800 for 2 h to activate the boron source. The integrated procedure avoided the annealed nickel foam from air, and shortened the experimental period to about 6 h.

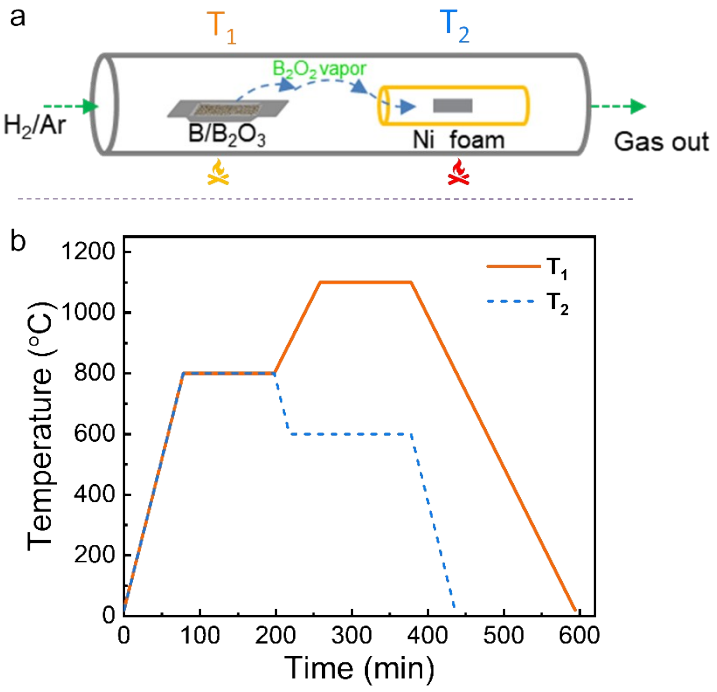

Figure S1 (a) CVD tubular furnace, and (b) Optimized growth temperature diagram of CVD tubular furnace with double temperature zone.

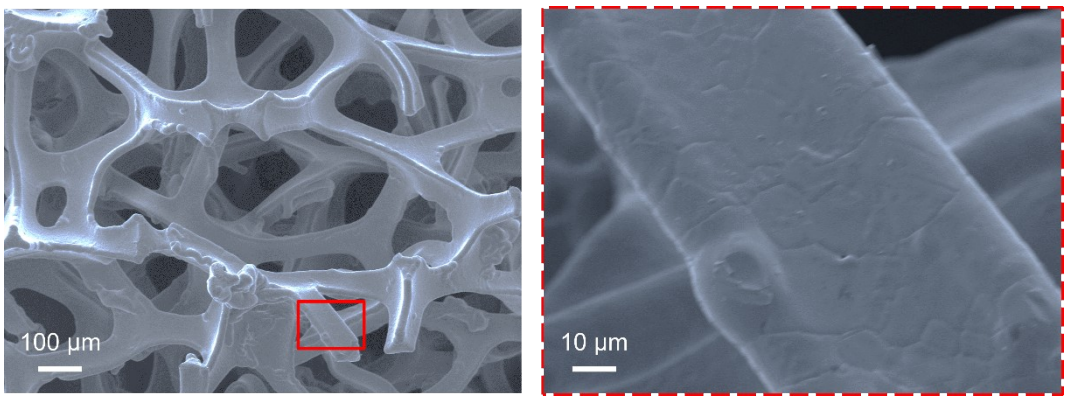

Figure S2 SEM images of the annealed nickel foam under Ar astomphere at 800 °C. For 2 h.

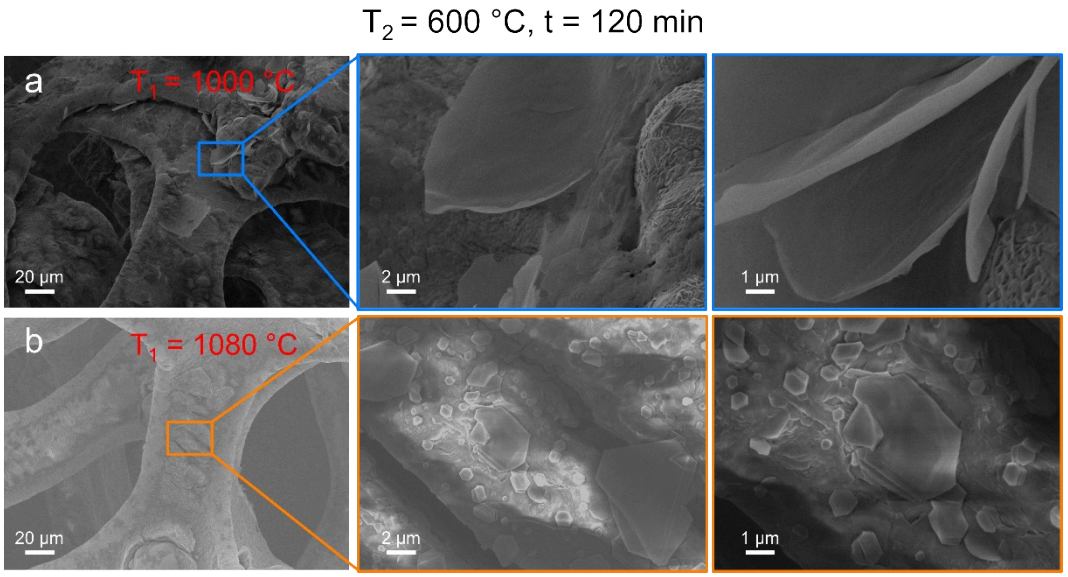

Figure S3 SEM images of annealed nickel foam at the temperature of 600 °C and the deposition time of 120 min in the T_2 zone, and different temperature in the T_1 zone. (a) 1000 °C, (b) 1080 °C.

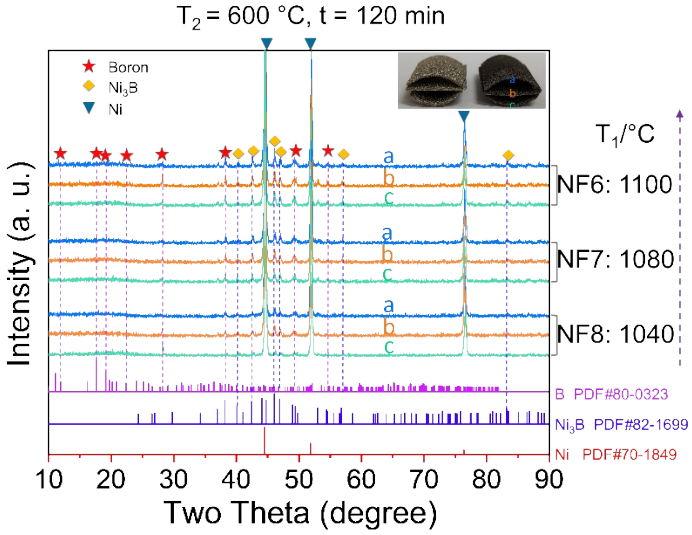

Figure S4 XRD patterns of three-layer nickel foam deposited with borophene sheets at the different temperatures of T_1 zone, the temperature of 600 °C and deposition time of 120 min in the T_2 zone.

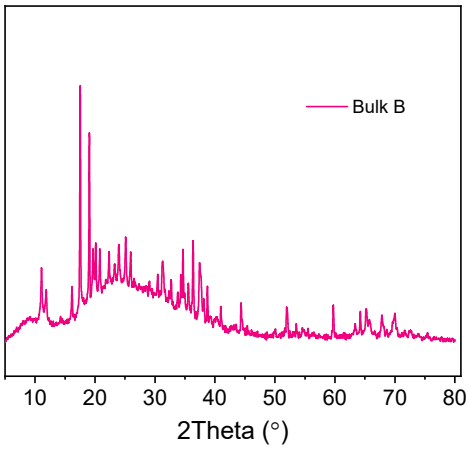

Figure S5 XRD patterns of the bulk boron.

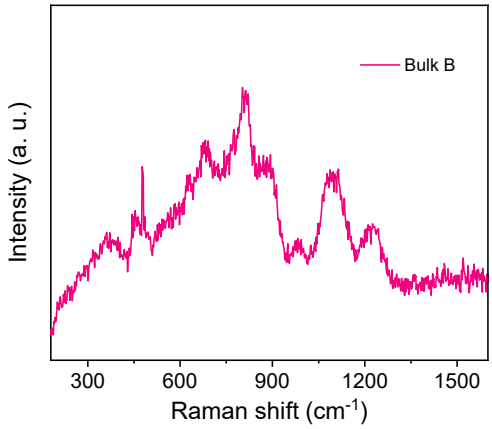

Figure S6 Raman spectroscopy of the bulk boron.

Table S1 Ratios of five types of B 1s components for NF8 and NF6.

No.	B—O		B—Ni		B—B	
	BE (eV)	Area (%)	BE (eV)	Area (%)	BE (eV)	Area (%)
NF8	195.1	59.67	193.2	39.6	187.3	0.74
NF6	194.7	78.70	193.6	18.85	187.8	2.44

Table S2 Ratios of five types of Ni 2p components for NF8 and NF6.

No.	Ni—B		Ni—Ni	
	BE (eV)	Area (%)	BE (eV)	Area (%)
NF8	852.0	68.38	869.3	31.62
NF6	852.8	66.82	870.1	33.18

Table S3 Charge/discharge capacity of as-prepared samples at 0.1 A g^{-1}.

Sample	Charge/Discharge capacity (mAh g^{-1})				ICE (%)
	1st cycle	2nd cycle	500th cycle	1000th cycle	
Blank NF	0.4/0.4	0.3/0.4	0.4/0.5	---	100
NF1	21/51	20/27	16/16	--	40.46
NF2	23/179	19/28	22/22	--	12.92
NF3	22/181	19/28	18/18	--	12.07
NF4	<1	<1	<1	--	--
NF5	25/110	22/29	23/23	--	22.90
NF6	5/24	3/4	2/2	--	20.42
NF7	7/33	7/9	4/4	3/3	19.90
NF8	3/6	3/4	7/7	10/10	50.00
NF9	5/40	5/7	4/4	3/3	12.78

Table S4 Kinetic parameters obtained by fitting an equivalent circuit.

Sample	R_s (ohm)	R_{ct} (ohm)
Blank NF	3.64	109
NF6	4.56	2243
NF8	3.25	3052

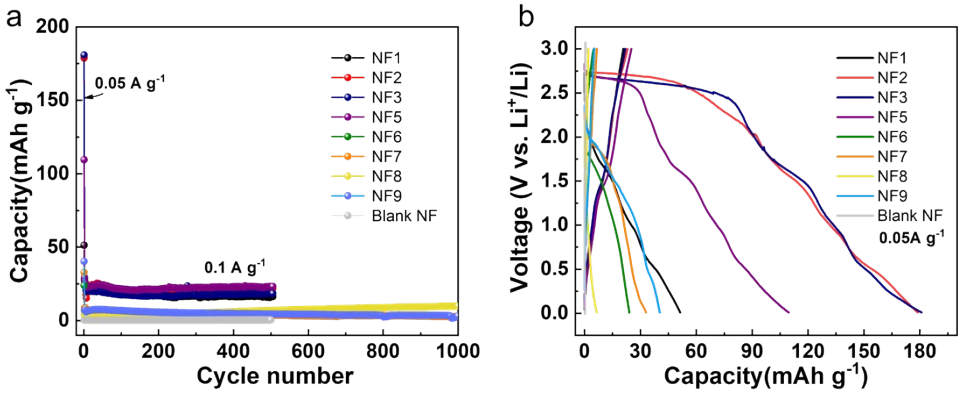

Figure S7 (a) Cyclic performance of as-fabricated electrodes at 0.1 A g^{-1} and (b) Charge-discharge profile of as-fabricated electrodes at 0.05 A g^{-1} for the first cycle.

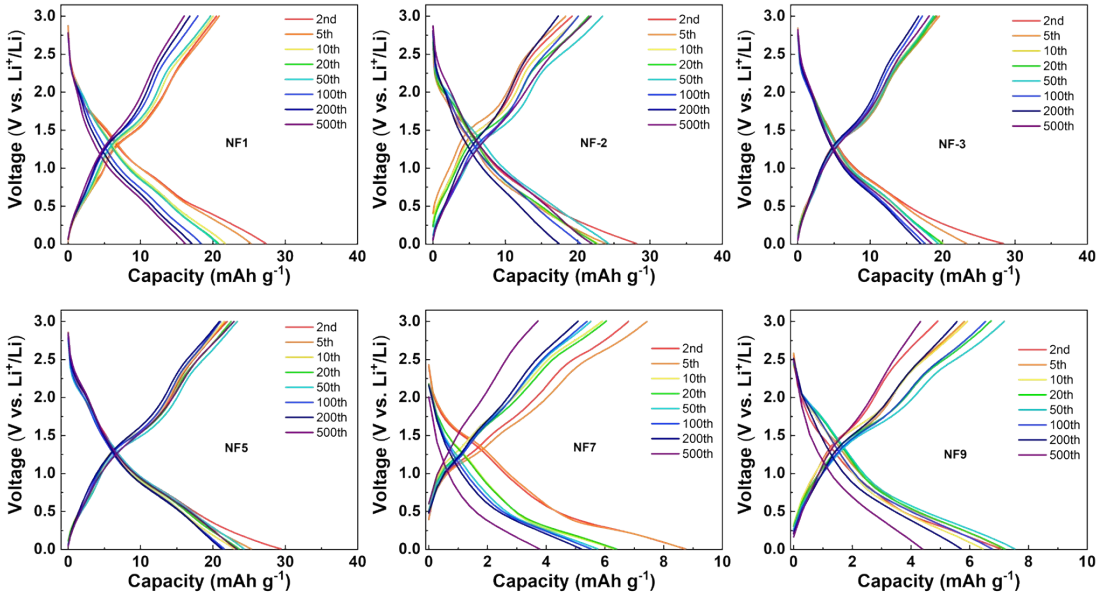

Figure S8 Charge-discharge profile of as-fabricated electrodes at 0.1 A g^{-1}.

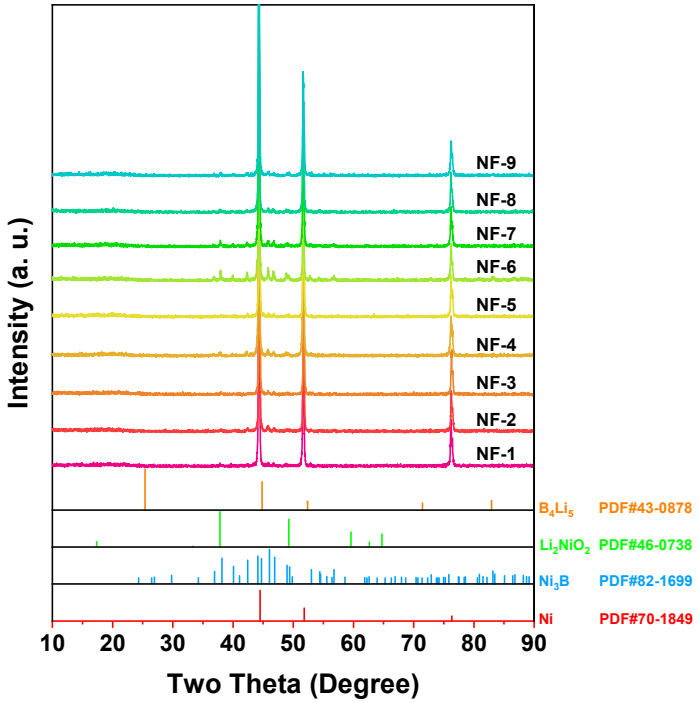

Figure S9 ex-situ XRD patterns of as-prepared samples after 500 charge-discharge cycles at 0.1 A g^{-1}.

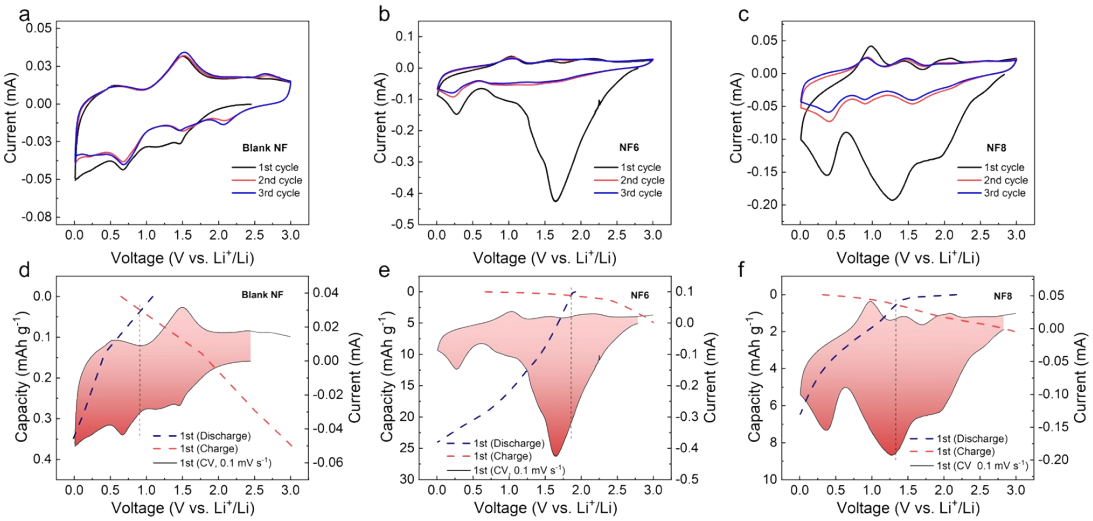

Figure S10 (a-c) CV curves at the scan rate of 0.1 mV s^{-1} over 3.0-0.01 V, and (d-f) Comparative analysis between CV curve and Charge-discharge profile for the first cycle of two representative (NF6, NF8) and blank NF electrodes.

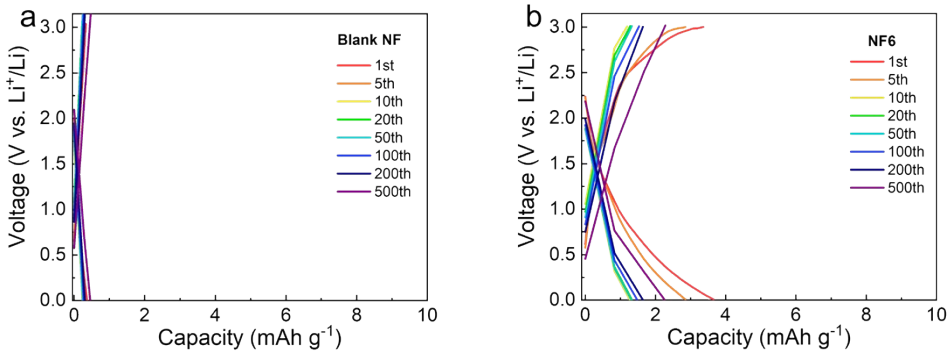

Figure S11 Charge-discharge profile of blank NF and NF6 electrodes at 0.1 A g^{-1}